

Time Crystals Protected by Floquet Dynamical Symmetry in Hubbard Models

Koki Chinzei and Tatsuhiko N. Ikeda

Institute for Solid State Physics, University of Tokyo, Kashiwa, Chiba 277-8581, Japan

(Dated: November 9, 2021)

We investigate an unconventional symmetry in time-periodically driven systems, the Floquet dynamical symmetry (FDS). Unlike the usual symmetries, the FDS does not give conserved quantities in the strict sense, but preserves some quantum coherence and leads to two kinds of time crystals: the commensurate and incommensurate time crystals that have different periodicity in time. We show that these time crystals appear in the Bose- and Fermi-Hubbard models under ac fields and their commensurability can be tuned only by adjusting the strength of the field. These time crystals arise only from the FDS and thus appear in both dissipative and isolated systems and in the presence of disorder as long as the FDS is respected. We discuss their experimental realizations in coldatom experiments and generalization to the $SU(N)$ -symmetric Hubbard models.

Introduction.— Symmetry is a key concept in physics, presenting us with various information such as conserved quantities, phase transitions and critical phenomena [1], and topological nature [2]. Even out of equilibrium, dynamics and nonequilibrium properties are governed by symmetries. In particular, (time-)periodically driven (Floquet) systems [3–5] involve novel symmetries without equilibrium counterparts due to the additional discrete time-translation symmetry, and these symmetries give rise to, for example, the Floquet (discrete) time crystals [6–20], Floquet symmetry protected topological phases [21–24], selection rules of high-harmonic generation in solids [25, 26], and so on.

Unlike the usual symmetries leading to the conserved quantities, there exist unconventional symmetries characterizing the nonequilibrium dynamics. The dynamical symmetry [27–31] in time-independent systems is one of them, ensuring the existence of a physical quantity that keeps oscillating periodically in time. This means the breaking of the continuous time-translation symmetry \mathbb{R} down to the discrete one characterized by integers \mathbb{Z} , leading to a time-crystalline state [27–29, 32–37]. The mechanism of this time crystal is different from the conventional Floquet time crystals, which occur in periodically driven systems. The Floquet time crystals are characterized by the breaking of the discrete time-translation symmetry \mathbb{Z} down to its subgroup such as $\mathbb{Z}/2$.

In this Letter, we investigate an unconventional symmetry in periodically driven systems, the Floquet dynamical symmetry (FDS), showing that the FDS governs the long-time behavior of the system. We show that the FDS protects quantum coherence between energetically-separated subspaces and leads to two kinds of time crystals: the commensurate and incommensurate time crystals (CTC and ITC) (the latter is also called as time quasicrystals [19]). These time crystals both break the discrete time-translation symmetry, but are different in that a perfect periodicity is retained or not (see Fig. 1). We show that these time crystals appear in various Hub-

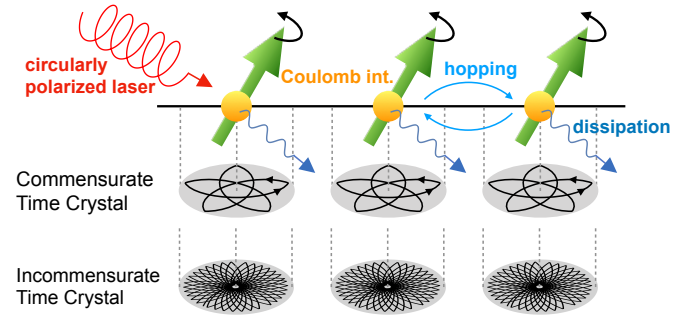


FIG. 1. Schematic illustration of time crystals in Hubbard model. The curves on the upper (lower) disks indicate the trajectories of the spin dynamics in the CTC (ITC) phase.

bard models under an ac field and their commensurability can be tuned only by adjusting the strength of the field.

Floquet dynamical symmetry and time crystals.— We begin by considering periodically-driven dissipative systems for a well-defined formulation, and will discuss isolated systems later. For this purpose, we focus on the Floquet-Lindblad master equation [38–41] ($\hbar = 1$ throughout this Letter):

$$\frac{d\rho}{dt} = \mathcal{L}_t(\rho) = -i[H(t), \rho] + \gamma \sum_k \left(L_k \rho L_k^\dagger - \frac{1}{2} \{L_k^\dagger L_k, \rho\} \right), \quad (1)$$

which describes trace-preserving nonunitary dynamics for the density matrix ρ . Here, $H(t) = H(t + T)$ is a time-periodic Hamiltonian describing the unitary part of the evolution, and L_k 's are the Lindblad operators representing the Markovian dissipation by an environment coupling to the system.

The solution of Eq. (1) is formally given by $\rho(t) = \mathcal{V}(t, 0)\rho(0)$, where $\mathcal{V}(t, t') \equiv \mathcal{T} \exp(\int_{t'}^t \mathcal{L}_s ds)$ is the time evolution superoperator from t' to t . Due to the periodicity of $\mathcal{L}_t = \mathcal{L}_{t+T}$, we can decompose $\mathcal{V}(t, 0)$ into a stroboscopic evolution and a micromotion: $\mathcal{V}(t, 0) = \mathcal{V}(\hat{t}, 0)\mathcal{U}_F^\ell$, where $t = \hat{t} + \ell T$ ($0 \leq \hat{t} < T$, $\ell \in \mathbb{N}$), and $\mathcal{U}_F = \mathcal{V}(T, 0)$

is the one-cycle time evolution superoperator. The long-time behavior ($\ell \rightarrow \infty$) is characterized by \mathcal{U}_F . If \mathcal{U}_F is diagonalizable $\mathcal{U}_F(\rho_j) = z_j \rho_j$ ($j = 1, \dots, D^2$ and D is the Hilbert-space dimension), the formal solution of Eq. (1) is given by $\rho(t) = \mathcal{V}(\tilde{t}, 0) \sum_j a_j z_j^\ell \rho_j$, where a_j is an expansion coefficients of $\rho(0) = \sum_j a_j \rho_j$. Note that the trace-preserving nature guarantees $|z_j| \leq 1$ and there exists at least one eigenvalue $z_j = 1$, and thus we set $z_1 = 1$ [42].

The unique nonequilibrium steady state (NESS) appears if all the other eigenvalues except $z_1 = 1$ satisfy $|z_{j \neq 1}| < 1$, meaning that $\rho_{j \neq 1}$ are all decaying modes with relaxation time $1/\ln|z_{j \neq 1}|$ [43]. In fact, any initial state asymptotically relax to a unique NESS, $\rho(t) = \mathcal{V}(\tilde{t}, 0) \sum_j a_j z_j^\ell \rho_j \xrightarrow{\ell \rightarrow \infty} \mathcal{V}(\tilde{t}, 0) \rho_1$ ($a_1 = 1$ due to the trace preservation). This NESS has time-period T by definition of $t = \tilde{t} + \ell T$, which means that the long-time behavior of Eq. (1) typically has the discrete time-translation symmetry \mathbb{Z} .

The conventional discrete time crystals [12–15] appear if there exist several eigenstates with eigenvalues $e^{i\theta}$ ($\theta = 2\pi/n, n \in \mathbb{N}$). For example, when $z_1 = 1$, $z_2 = -1$, and $|z_{j \neq 1, 2}| < 1$, any initial state asymptotically relax to the following NESS: $\rho(t) = \mathcal{V}(\tilde{t}, 0) \sum_j a_j z_j^\ell \rho_j \xrightarrow{\ell \rightarrow \infty} \mathcal{V}(\tilde{t})[\rho_1 + (-1)^\ell a_2 \rho_2]$. When $a_2 \neq 0$, the NESS is a time-crystalline state with time-period $2T$, which implies $\mathbb{Z} \rightarrow \mathbb{Z}/2$ symmetry breaking. From now on, we call the eigenstate with eigenvalue 1 as a steady state, and that with eigenvalue $e^{i\theta}$ ($\theta \in \mathbb{R}$) as a coherent state.

Now we introduce the Floquet dynamical symmetry (FDS), which leads to unconventional time crystals. First, we define the FDS for \mathcal{U}_F by

$$\begin{aligned} \mathcal{U}_F(A\rho) &= e^{-i\lambda T} A \mathcal{U}_F(\rho), \quad \forall \rho \\ \mathcal{U}_F(\rho A^\dagger) &= e^{i\lambda T} \mathcal{U}_F(\rho) A^\dagger, \quad \forall \rho \end{aligned} \quad (2)$$

where A is a dynamical symmetry operator, and λ is a real number. This definition is a natural extension of the strong dynamical symmetry in time-independent systems [27, 29], which is defined as $[H, A] = \lambda A$ and $[L_k, A] = [L_k^\dagger, A] = 0$ (e.g., the Zeeman Hamiltonian $H = \lambda S^z$ and the raising operator $A = S^+$ satisfy this relation, $[H, A] = \lambda A$). One can easily show that, in the Floquet systems, when the strong dynamical symmetry holds at any time, there exists the FDS, but the converse is not true. We note that the dissipation L_k is not required for the FDS, and the time crystals can appear even in isolated systems as we will show later.

The FDS protects some quantum coherence, and prevents the quantum state from relaxing to the unique NESS. Given that ρ_s is a steady state satisfying $\mathcal{L}\rho_s = \rho_s$, $\rho_{mn} = A^m \rho_s (A^\dagger)^n$ are the steady ($m = n$) and coherent ($m \neq n$) states,

$$\mathcal{U}_F(\rho_{mn}) = e^{i(n-m)\lambda T} \rho_{mn}. \quad (3)$$

If there are no other steady and coherent states except ρ_{mn} , we obtain the long-time behavior from them,

$$\rho(t) \xrightarrow{\ell \rightarrow \infty} \sum_{mn} \mathcal{V}(\tilde{t}, 0) [c_{mn} e^{i(n-m)\lambda \ell T} \rho_{mn}] \equiv \rho_\infty(t), \quad (4)$$

where c_{mn} is expansion coefficients of ρ_{mn} . There exist two typical energy (time) scales in $\rho_\infty(t)$. One is the Floquet frequency $\omega = 2\pi/T$ stemming from the periodicity of $\mathcal{V}(\tilde{t}, 0)$, and the other is λ characterized by the FDS.

Depending on whether the ratio λ/ω is a rational number or not, the long-time behavior (4) represents the CTC or ITC, respectively. If $\lambda/\omega \in \mathbb{Q}$, i.e., $\lambda/\omega = q/p$ for some coprime integers p (≥ 2) and q , the CTC emerges: $\rho_\infty(t+T) \neq \rho_\infty(t)$, but $\rho_\infty(t+pT) = \rho_\infty(t)$ holds true. This means the discrete time-translation symmetry breaking, $\mathbb{Z} \rightarrow \mathbb{Z}/p$. On the other hand, if $\lambda/\omega \notin \mathbb{Q}$, the discrete time-translation symmetry \mathbb{Z} is broken, but there is no integer p such that $\rho_\infty(t+pT) = \rho_\infty(t)$. Nevertheless, there exist an infinite number of times s such that $\rho_\infty(t+s)$ is arbitrarily close to $\rho_\infty(t)$. Thus, the dynamics is quasiperiodic, and we call it the ITC.

Tunable time crystals in dissipative Hubbard models.— Here we present simple models exhibiting the time crystals protected by the FDS: spin- S Bose- or Fermi-Hubbard models driven by a circularly polarized ac field in d dimensions. The Hamiltonian $H(t) = H_0 + V(t)$ is given by

$$\begin{aligned} H_0 &= -J \sum_{\langle i,j \rangle, \sigma} (c_{i,\sigma}^\dagger c_{j,\sigma} + \text{h.c.}) + \frac{U}{2} \sum_j n_j^2 + \frac{K}{2} \sum_{\langle i,j \rangle} n_i n_j, \\ V(t) &= B (S^x \cos \omega t + S^y \sin \omega t), \end{aligned} \quad (5)$$

where $c_{j,\sigma}$ ($c_{j,\sigma}^\dagger$) is the annihilation (creation) operator for the boson or fermion with spin $\sigma \in \{-S, \dots, S\}$ on the site j , and $n_j = \sum_\sigma c_{j,\sigma}^\dagger c_{j,\sigma}$ is the particle number operator. The operators for the spin at site j and for the total spin are denoted by S_j^μ and $S^\mu = \sum_j S_j^\mu$ ($\mu = x, y, z$). The strength of the hopping amplitude, the onsite interaction, and the nearest neighbor interaction are denoted by J , U , and K , respectively. The nearest neighbor interaction is added to elucidate below that our results do not rely on the integrability. In the ac Zeeman coupling term $V(t)$, B and ω are the strength and frequency of the magnetic field, respectively [44].

We assume that the dissipation is described by local dephasing Lindblad operators acting on each site, $L_j = n_j$, which suppresses the particle number fluctuation. We will discuss later how to realize them experimentally.

Our model has the FDS in one cycle of the ac field. To show this, we consider a unitary transformation to the rotating frame [45–47], $\rho_{\text{RF}}(t) = R(t)\rho(t)R(t)^\dagger$ ($R(t) = e^{i\omega t S^z}$). Then, the Hamiltonian is transformed to the Hubbard model in an effective static magnetic field, $H_{\text{RF}} = R(t)[H(t) - i\partial_t]R(t)^\dagger = H_0 + \mathbf{h} \cdot \mathbf{S}$,

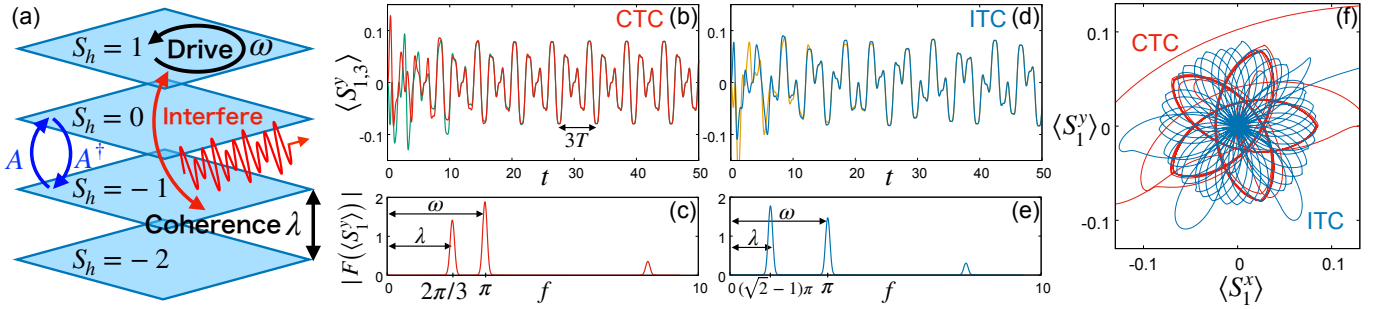


FIG. 2. (a) Mechanism of time crystals by Floquet dynamical symmetry. Each sheet represents the different spin sectors. The time-periodic drive and the quantum coherence interfere with each other. (b) Time evolutions of $\langle S_j^y(t) \rangle$ (red: $j = 1$, green: $j = 3$) in the CTC phase, and (c) the Fourier component ($j = 1$). (d) Time evolutions of $\langle S_j^y(t) \rangle$ (blue: $j = 1$, orange: $j = 3$) in the ITC phase, and (e) the Fourier component ($j = 1$). We have performed the Fourier transformation for $t \in [20, 100]$ by convoluting the window function $w(t) = \exp[-(t - 60)^2/20^2]$. (f) Trajectories of time evolution in xy -spin plane. The red (blue) curve denotes the CTC (ITC) trajectory. The parameters are $J = U = K = 1, \omega = \pi$, and $B = 4\pi/3$ for the CTC case ($B = \pi$ for the ITC case). The system size is $L = 6$.

where $\mathbf{h} = (B, 0, \omega)$, while the Lindblad operators are invariant. Therefore, in the rotating frame, the system has the strong dynamical symmetry [27, 29], or the FDS $\mathcal{U}_F^{\text{RF}}(A\rho) = e^{-i\lambda T} A \mathcal{U}_F^{\text{RF}}(\rho)$ and $\mathcal{U}_F^{\text{RF}}(\rho A^\dagger) = e^{i\lambda T} \mathcal{U}_F^{\text{RF}}(\rho) A^\dagger$, where $\mathcal{U}_F^{\text{RF}}$ is the one-cycle time evolution superoperator in the rotating frame, $A = S_{\mathbf{h}}^+$ is the total spin raising operator along the effective magnetic field \mathbf{h} , and

$$\lambda = |\mathbf{h}| = \sqrt{\omega^2 + B^2} \pmod{\omega}. \quad (6)$$

Going back to the original frame, we have $\mathcal{U}_F(\rho) = R^\dagger(T) \mathcal{U}_F^{\text{RF}}[R(0)\rho R(0)^\dagger] R(T) = \mathcal{U}_F^{\text{RF}}(\rho)$ due to $R(0) = 1$ and $R(T) = (-1)^{2SV}$ (V is the total number of sites), obtaining the FDS

$$\begin{aligned} \mathcal{U}_F(S_{\mathbf{h}}^+ \rho) &= e^{-i\lambda T} S_{\mathbf{h}}^+ \mathcal{U}_F(\rho), \quad \forall \rho \\ \mathcal{U}_F(\rho S_{\mathbf{h}}^-) &= e^{i\lambda T} \mathcal{U}_F(\rho) S_{\mathbf{h}}^-. \quad \forall \rho \end{aligned} \quad (7)$$

We note that the symmetry operator $A = S_{\mathbf{h}}^+$ depends on the time origin t_0 , which has been set to 0 above, and is generally given by $A(t_0) = S_{\mathbf{h}(t_0)}^+$ with $\mathbf{h}(t_0) = (B \cos \omega t_0, B \sin \omega t_0, \omega)$.

This FDS gives the steady and coherent states $\rho_{mn} = (S_{\mathbf{h}}^+)^m \rho_s (S_{\mathbf{h}}^-)^n$ with eigenvalue $e^{i(n-m)\lambda T}$ in Eq. (3). This implies that the FDS protects the coherence between the different spin sectors labelled by $S_{\mathbf{h}} = \mathbf{h} \cdot \mathbf{S} / |\mathbf{h}|$, which are Zeeman-split by λ (see Fig. 2 (a)). Furthermore, the system has another intrinsic energy scale ω of the drive frequency. These two scales, ω and λ , interfere with each other and give rise to the CTC and ITC.

We emphasize the tunability of our time crystals. As shown before, the commensurability and the period of these time crystals depend on the ratio $\lambda/\omega = \sqrt{1 + (B/\omega)^2}$, which can be tuned only by varying the field strength B with ω fixed. If $\lambda/\omega = q/p$ ($\leftrightarrow B =$

$\omega \sqrt{(q/p)^2 - 1}$) with coprime integers p and q , the CTC appears with period pT , whereas, if $\lambda/\omega \notin \mathbb{Q}$, the ITC appears.

Synchronized CTC and ITC in the Hubbard model.— Let us numerically demonstrate the CTC and ITC by taking the spin-1/2 Fermi-Hubbard model in one dimension with L sites. We assume the periodic boundary condition. Throughout this Letter, the initial state is a 1/4-filled state where the j -th site ($j = 1, 2, \dots, L/2$) is occupied by one fermion, and every third fermions are polarized along $-x$ and all others are polarized along x (we assume L is a multiple of 6).

Figure 2 (b) shows the time evolution of $\langle S_j^y(t) \rangle$ ($j = 1, 3$) in the CTC phase for $\omega = \pi$ and $\lambda = 2\pi/3$. After the initial relaxation dynamics, $\langle S_j^y(t) \rangle$ oscillates with period $3T = 6$, which is the least common multiple of $T = 2\pi/\omega = 2$ and $2\pi/\lambda = 3$. This means the discrete time-translation symmetry breaking $\mathbb{Z} \rightarrow \mathbb{Z}/3$. Moreover, the dynamics of $\langle S_1^y(t) \rangle$ and $\langle S_3^y(t) \rangle$ are synchronized after relaxation, which implies all the steady and coherent states are translationally symmetric [27, 29]. The Fourier component of $\langle S_1^y(t) \rangle$ is shown in Fig. 2 (c), where there exist two sharp peaks at $f = \omega$ and λ . The rationality of the two peaks, $f = \omega$ and λ , leads to the commensurability of the time crystal.

On the other hand, Fig. 2 (d) shows the time evolution in the ITC phase for $\omega = \pi$ and $\lambda = (\sqrt{2} - 1)\pi$. As shown in the figure, the synchronized spin dynamics oscillate aperiodically. The irrationality of two peaks, $f = \omega$ and λ , in the Fourier space (Fig. 2 (e)) shows the incommensurability of the time crystal and no perfect periodicity.

The trajectories of the CTC and ITC dynamics in the (S_1^x, S_1^y) -plane are shown in Fig. 2 (f). The trajectory of the CTC dynamics (red) behaves as the limit cycle, and gradually converges to the star-shaped closed curve.

On the other hand, the trajectory of the ITC dynamics (blue) never converges to a closed curve, and keep rotating aperiodically on the plane. This aperiodic dynamics highlights the difference from the CTC.

Quantum-thermalization-induced time crystals without dissipation.— Until now, we have considered the dissipative systems to clarify the role of the FDS and the mechanism of the time crystals. However, the time crystals do not necessarily require the dissipation. According to the recent studies [48–50], an isolated quantum system without dissipation exhibits thermalization if nonintegrable. Here we show that the CTC and ITC protected by the FDS also occur in the isolated Hubbard model due to this quantum thermalization.

Figures 3 (a) and (b) shows the results without the dissipation for $\omega = \pi$ and $\lambda = 2\pi/3$. In contrast to the non-interacting (integrable) case (Fig. 3 (b)), in the interacting (nonintegrable) case (Fig. 3 (a)), the spin dynamics at the different sites are synchronized, and the time crystal appears. The quantum thermalization effectively plays the role of dissipation and eliminates quantum coherence except those protected by the FDS, bringing about the time crystals.

These synchronized time crystals in isolated systems are interpreted by the maximum entropy principle under multiple conserved quantities [51] that is also known as the generalized Gibbs ensemble (GGE) [52] [53]. The key to this interpretation is the unconventional conserved quantities that are derived from the dynamical symmetry and conserved only stroboscopically [28]. In the rotating frame, one can easily show that $S_{\mathbf{h}}^{\pm}$ are such quantities: $S_{\mathbf{h}}^{\pm}(s + nT_{\lambda}) = S_{\mathbf{h}}^{\pm}(s)$ in the Heisenberg picture for each $s \in [0, T_{\lambda})$ with $T_{\lambda} = 2\pi/\lambda$ and $n \in \mathbb{N}$. Thus, each stroboscopic evolution from $t = s$ leads, after a long time, to the GGE characterized by $S_{\mathbf{h}}^{\pm}$: $\rho_{\text{RF}}(t) = \exp[-\sum_j \beta_j Q_j - \mu(t) S_{\mathbf{h}}^+ - \mu(t)^* S_{\mathbf{h}}^-]/Z_t$. Here $Z_t = Z_{t+T_{\lambda}}$ is the periodic partition function, $\mu(t) = \mu(t + T_{\lambda})$ is the periodic chemical potential for $S_{\mathbf{h}}^+$, and Q_i and β_i are the conventional (not stroboscopic) local conserved quantities and their generalized inverse temperatures. The noncommutativity between the conserved quantities does not affect the foundation of the GGE [54–56]. Going back to the original frame, we obtain a time-dependent GGE $\rho_{\text{TC}}(t) = R^{\dagger}(t)\rho_{\text{RF}}R(t)$ as follows:

$$\rho_{\text{TC}}(t) = \frac{\exp\left[-\sum_i \beta_i Q_i(t) - \mu(t) S_{\mathbf{h}(t)}^+ - \mu(t)^* S_{\mathbf{h}(t)}^-\right]}{Z_t}, \quad (8)$$

where $Q_i(t) = R^{\dagger}(t)Q_iR(t)$ and $S_{\mathbf{h}(t)}^{\pm} = R^{\dagger}(t)S_{\mathbf{h}}^{\pm}R(t)$ (see also below Eq. (7)).

The time-dependent GGE (8) is a two-color generalization of the previous ones [28, 57]. Whereas $Q_i(t)$ and $S_{\mathbf{h}(t)}^{\pm}$ have the period $T = 2\pi/\omega$ of the external field, $\mu(t)$

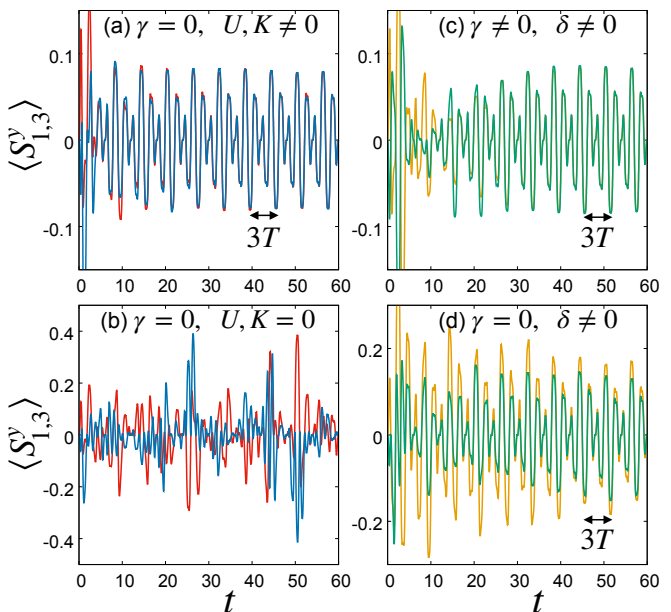


FIG. 3. (a,b) Time evolution of $\langle S_j^y \rangle$ (red: $j = 1$, blue: $j = 3$) in Hubbard model without dissipation for (a) $U = K = 1$ and (b) $U = K = 0$. (c,d) Time evolution of $\langle S_j^y \rangle$ (orange: $j = 1$, green: $j = 3$) in Hubbard model with disorder $\delta = 3$ and interaction $U = K = 1$ for (c) $\gamma = 0.1$ and (d) $\gamma = 0$. The parameters are $J = 1, \omega = \pi$, and $B = 4\pi/3$. The system sizes are $L = 6$ for (c) and $L = 12$ for (a), (b), and (d).

has a different one $T_{\lambda} = 2\pi/\lambda$ of the FDS. These two periods, depending on their ratio, give the CTC and ITC in isolated systems. The synchronization derives from the translation symmetry of $Q_i(t)$ and $S_{\mathbf{h}(t)}^{\pm}$.

Robustness against disorder.— Finally, we show that the time-crystalline nature is robust against perturbations as long as the FDS is preserved, although the synchronization may become imperfect. To illustrate this, we consider the disordered onsite potential $V_d = \sum_j \epsilon_j n_j$, where ϵ_j 's are independent random variables following the uniform distribution over $(-\delta, \delta)$. This disorder respects the FDS due to the spin-SU(2) symmetry, but breaks the spatial translation symmetry.

In the presence of the dissipation $L_j = n_j$, not only the time-crystalline nature but also the synchronization are robust against the disorder. Figure 3 (c) shows the dynamics of $\langle S_j^y \rangle$ ($j = 1, 3$) in the disordered Hubbard model with dissipation for the CTC phase, $\omega = \pi$ and $\lambda = 2\pi/3$, and thus the period is $3T$. As in the case without disorder (Fig. 2 (b)), the two spin dynamics become synchronized to oscillate with period $3T$. This synchronization is caused by the dissipation $L_j = n_j$ suppressing the particle number fluctuations to realize the translationally symmetric state.

On the other hand, in the absence of dissipation, the perfect synchronization does not occur, but the time-

crystalline nature persists. Figure 3 (d) shows the dynamics of $\langle S_j^y \rangle$ ($j = 1, 3$) in the disordered Hubbard model without dissipation for the CTC phase with period $3T$. Unlike the dissipative system, the amplitudes of the two spin dynamics are different and have fluctuations in time. However, the rhythms of the oscillations are synchronized, and the time crystal with period $3T$ appears. This spatial inhomogeneity can be understood by the quantum thermalization. Since a state thermalizes to an equilibrium state of the disordered Hamiltonian, the realized state is not translationally symmetric.

Discussions and conclusions.— In this Letter, we have introduced the FDS and proposed a new class of time crystals protected by the FDS. In this class, the time-crystalline nature is determined only by the FDS and robust against perturbations respecting the symmetry. We also have demonstrated that in the Hubbard model driven by the circularly polarized ac field.

The time crystals also appear in the Hubbard model with a static and linearly polarized ac fields both along the z -direction. This is because a trivial dynamical symmetry holds at any time, $[H(t), S^+] \propto S^+$. This setup is known as the electron spin resonance (ESR) in the condensed matter physics [58].

Our model (5) can be realized in ultracold atoms on an optical lattice [59, 60]. The hyperfine states of the atom behave as a pseudospin, and the coupling between the states, or the Zeeman effect on the pseudospin, is manipulated by radio waves [60]. State-of-the-art laser technology enables us to control the strength and frequency of the coupling, realizing the highly tunable time crystals. Also, the particle number dephasing $L_j = n_j$ is achieved by immersing the optical lattice into a Bose-Einstein condensate [61, 62].

Finally, we note that our model (5) actually has the $SU(N)$ symmetry with $N = 2S + 1$ [63–65]. Such an $SU(N)$ -symmetric Hubbard model has been realized in ultracold atoms [66–68], and has attracted much attention recently. Generalizing our rotating-frame arguments to the $SU(N)$ algebra is an interesting open question, where time crystals should meet large Lie algebras together with coldatom experiments.

Acknowledgements.— We thank H. Tsunetsugu for fruitful discussions. This work was supported by JSPS KAKENHI Grant No. JP18K13495. K. C. acknowledges the financial support provided by the Advanced Leading Graduate Course for Photon Science at the University of Tokyo.

Note added.— In preparing this manuscript, we have become aware of an independent work [30], where the FDS and its consequences are briefly discussed.

-
- [1] J. Cardy, *Scaling and Renormalization in Statistical Physics* (Cambridge Lecture Notes in Physics Book 5, 1996).
 - [2] T. Senthil, Annual Review of Condensed Matter Physics **6**, 299 (2015).
 - [3] Martin Holthaus, Journal of Physics B: Atomic, Molecular and Optical Physics **49**, 013001 (2015).
 - [4] M. Bukov, L. D’Alessio, and A. Polkovnikov, Advances in Physics **64**, 139 (2015).
 - [5] T. Oka and S. Kitamura, Annual Review of Condensed Matter Physics **10**, 387 (2019).
 - [6] D. V. Else, B. Bauer, and C. Nayak, Physical Review Letters **117**, 090402 (2016).
 - [7] C. W. Von Keyserlingk, V. Khemani, and S. L. Sondhi, Physical Review B **94**, 085112 (2016).
 - [8] N. Y. Yao, A. C. Potter, I. D. Potirniche, and A. Vishwanath, Physical Review Letters **118**, 030401 (2017).
 - [9] D. V. Else, B. Bauer, and C. Nayak, Physical Review X **7**, 011026 (2017).
 - [10] T. S. Zeng and D. N. Sheng, Physical Review B **96**, 094202 (2017).
 - [11] K. Mizuta, K. Takasan, M. Nakagawa, and N. Kawakami, Physical Review Letters **121**, 093001 (2018).
 - [12] Z. Gong, R. Hamazaki, and M. Ueda, Physical Review Letters **120**, 040404 (2018).
 - [13] D. Barberena, R. J. Lewis-Swan, J. K. Thompson, and A. M. Rey, Physical Review A **99**, 053411 (2019).
 - [14] C. Lledó, T. K. Mavrogordatos, and M. H. Szymańska, Physical Review B **100**, 054303 (2019).
 - [15] A. Riera-Campeny, M. Moreno-Cardoner, and A. Sanpera, arXiv:1908.11339 (2019).
 - [16] K. Sacha, Physical Review A - Atomic, Molecular, and Optical Physics **91**, 033617 (2015).
 - [17] A. Russomanno, F. Iemini, M. Dalmonte, and R. Fazio, Physical Review B **95**, 214307 (2017).
 - [18] W. W. Ho, S. Choi, M. D. Lukin, and D. A. Abanin, Physical Review Letters **119**, 010602 (2017).
 - [19] A. Pizzi, J. Knolle, and A. Nunnenkamp, Physical Review Letters **123**, 150601 (2019).
 - [20] K. Giergiel, A. Dauphin, M. Lewenstein, J. Zakrzewski, and K. Sacha, New Journal of Physics **21**, 052003 (2019).
 - [21] T. Kitagawa, E. Berg, M. Rudner, and E. Demler, Physical Review B **82**, 235114 (2010).
 - [22] L. Jiang, T. Kitagawa, J. Alicea, A. R. Akhmerov, D. Pekker, G. Refael, J. I. Cirac, E. Demler, M. D. Lukin, and P. Zoller, Physical Review Letters **106**, 220402 (2011).
 - [23] M. S. Rudner, N. H. Lindne, E. Berg, and M. Levin, Physical Review X **3**, 031005 (2013).
 - [24] A. C. Potter, T. Morimoto, and A. Vishwanath, Physical Review X **6**, 041001 (2016).
 - [25] O. E. Alon, V. Averbukh, and N. Moiseyev, Physical Review Letters **80**, 3743 (1998).
 - [26] O. Neufeld, D. Podolsky, and O. Cohen, Nature Communications **10**, 405 (2019).
 - [27] B. Buča, J. Tindall, and D. Jaksch, Nature Communications **10**, 1730 (2019).
 - [28] M. Medenjak, B. Buča, and D. Jaksch, arXiv:1905.08266 (2019).

- [29] J. Tindall, C. Sánchez Muñoz, B. Buča, and D. Jaksch, *New Journal of Physics* **22**, 013026 (2020).
- [30] M. Medenjak, T. Prosen, and L. Zadnik, arXiv:2003.01035 (2020).
- [31] Carlos Sánchez Muñoz, B. Buča, J. Tindall, A. González-Tudela, D. Jaksch, and D. Porrás, *Physical Review A* **100**, 042113 (2019).
- [32] F. Wilczek, *Physical Review Letters* **109**, 160401 (2012).
- [33] T. Li, Z.-X. Gong, Z.-Q. Yin, H. T. Quan, X. Yin, P. Zhang, L.-M. Duan, and X. Zhang, *Physical Review Letters* **109**, 163001 (2012).
- [34] P. Bruno, *Physical Review Letters* **110**, 118901 (2013).
- [35] P. Bruno, *Physical Review Letters* **111**, 29301 (2013).
- [36] H. Watanabe and M. Oshikawa, *Physical Review Letters* **114**, 251603 (2015).
- [37] K. Nakatsugawa, T. Fujii, and S. Tanda, *Physical Review B* **96**, 94308 (2017).
- [38] T.-S. Ho, K. Wang, and S.-I. Chu, *Physical Review A* **33**, 1798 (1986).
- [39] T. Prosen and E. Ilievski, *Physical Review Letters* **107**, 60403 (2011).
- [40] D. Vorberg, W. Wustmann, R. Ketzmerick, and A. Eckardt, *Phys. Rev. Lett.* **111**, 240405 (2013).
- [41] M. Hartmann, D. Poletti, M. Ivanchenko, S. Denisov, and P. Hänggi, *New Journal of Physics* **19**, 83011 (2017).
- [42] H. P. Breuer and F. Petruccione, *The theory of open quantum systems* (Oxford University Press, Great Clarendon Street, 2002).
- [43] T. N. Ikeda and M. Sato, arXiv:2003.02876 (2020).
- [44] We ignore the coupling between the electric field and electric charges for simplicity. If included, this coupling does not change the results qualitatively since it does not affect the spin dynamics.
- [45] C. P. Slichter, *Principles of Magnetic Resonance*, 3rd ed. (Springer, 1996).
- [46] S. Kohler, J. Lehmann, and P. Hänggi, *Physics Reports* **406**, 379 (2005).
- [47] S. Takayoshi, M. Sato, and T. Oka, *Physical Review B* **90**, 214413 (2014).
- [48] L. D'Alessio, Y. Kafri, A. Polkovnikov, and M. Rigol, *Advances in Physics* **65**, 239 (2016).
- [49] J. Eisert, M. Friesdorf, and C. Gogolin, *Nature Physics* **11**, 124 (2015).
- [50] T. Mori, T. N. Ikeda, E. Kaminishi, and M. Ueda, *Journal of Physics B: Atomic, Molecular and Optical Physics* **51**, 112001 (2018).
- [51] E. Jaynes, *Physical Review* **106**, 620 (1957).
- [52] M. Rigol, V. Dunjko, V. Yurovsky, and M. Olshanii, *Physical Review Letters* **98**, 050405 (2007).
- [53] The terminology GGE is sometimes limited to the case when there exists an extensive number of conserved quantities, unlike our model.
- [54] M. Fagotti, *Journal of Statistical Mechanics: Theory and Experiment* **2014**, P03016 (2014).
- [55] N. Yunger Halpern, M. E. Beverland, and A. Kalev, (2019), arXiv:1906.09227.
- [56] K. Fukai, Y. Nozawa, K. Kawahara, and T. N. Ikeda, arXiv:2003.00022 (2020).
- [57] A. Lazarides, A. Das, and R. Moessner, *Physical Review Letters* **112**, 1 (2014).
- [58] A. J. Weil, *Physics and Chemistry of Minerals* **10**, 149 (1984).
- [59] D. Jaksch and P. Zoller, *Annals of Physics* **315**, 52 (2005).
- [60] T. Esslinger, *Annual Review of Condensed Matter Physics* **1**, 129 (2010).
- [61] A. Klein, M. Bruderer, S. R. Clark, and D. Jaksch, *New Journal of Physics* **9**, 411 (2007).
- [62] D. Mayer, F. Schmidt, D. Adam, S. Haupt, J. Koch, T. Lausch, J. Nettersheim, Q. Bouton, and A. Widera, *Journal of Physics B: Atomic, Molecular and Optical Physics* **52**, 015301 (2019).
- [63] C. Honerkamp and W. Hofstetter, *Physical Review Letters* **92**, 170403 (2004).
- [64] M. A. Cazalilla, A. F. Ho, and M. Ueda, *New Journal of Physics* **11**, 103033 (2009).
- [65] A. V. Gorshkov, M. Hermele, V. Gurarie, C. Xu, P. S. Julienne, J. Ye, P. Zoller, E. Demler, M. D. Lukin, and A. M. Rey, *Nature Physics* **6**, 289 (2010).
- [66] S. Taie, Y. Takasu, S. Sugawa, R. Yamazaki, T. Tsujimoto, R. Murakami, and Y. Takahashi, *Physical Review Letters* **105**, 190401 (2010).
- [67] X. Zhang, M. Bishof, S. L. Bromley, C. V. Kraus, M. S. Safronova, P. Zoller, A. M. Rey, and J. Ye, *Science* **345**, 1467 LP (2014).
- [68] F. Scazza, C. Hofrichter, M. Höfer, P. C. D. Groot, I. Bloch, and S. Fölling, *Nature Physics* **10**, 779 (2014).